AD-A157 914 STRAIN ENERGY DENSITY CRITERIA FOR DYNAMIC FRACTURE AND DYNAMIC CRACK BRA..(U) WASHINGTON UNIV SEATTLE DEPT OF MECHANICAL ENGINEERING M RAMULU ET AL. JUL 85 1/1

UNCLASSIFIED UWA/DME/TR-85/51 N00014-85-K-0187 F/G 20/11 NL

END

FILMED

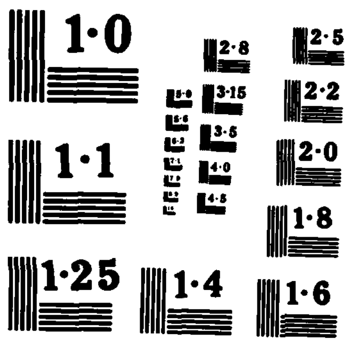
1·0
2·8
2·5
3·15
2·2
3·5
1·1
2·0
4·0
4·5
1·8
1·25
1·4
1·6

Office of Naval Research

Contract N00014-85-K-0187

Technical Report No. UWA/DME/TR-85/51

STRAIN ENERGY DENSITY CRITERIA FOR DYNAMIC FRACTURE AND DYNAMIC CRACK BRANCHING

by

M. Ramulu and A. S. Kobayashi

July 1985

The research reported in this technical report was made possible through support extended to the Department of Mechanical Engineering, University of Washington, by the Office of Naval Research under Contract N00014-85-K-0187. Reproduction in whole or in part is permitted for any purpose of the United States Government.

Department of Mechanical Engineering

College of Engineering

University of Washington

STRAIN ENERGY DENSITY CRITERIA FOR DYNAMIC FRACTURE AND DYNAMIC CRACK BRANCHING

M. Ramulu and A.S. Kobayashi
Department of Mechanical Engineering
University of Washington, FU-10
Seattle, Washington 98195

ABSTRACT

Dynamic extension of Sih's fracture criterion based on strain energy density factor, r_c(dW/dV), is used to analyze dynamic crack propagation and branching. Influence of the nonsingular components, which are known as the higher order terms (HOT) in the crack tip stress field, on the strain energy density distribution at a critical distance surrounding the crack tip moving at constant crack velocity is examined. This r_c(dW/dV) fracture criterion is then used to analyze available dynamic photoelastic results of crack branching and of engineering materials.

INTRODUCTION

The mechanics associated with the curved crack paths or bifurcation events received continuous attention in the literature. Comprehensive reviews on crack curving and branching were published by the authors [1] and Dally [2]. Literature on crack branching during rapid fracture discusses its correlation with either the dynamic crack tip stress field, initiation of secondary cracks, or with stress wave loading. These studies deal primarily with the stress intensity factor, the strain energy release rate at the instant of branching and the branching crack velocity. The crack branching angle as well as the crack curving angle can also be determined by a crack directional stability criteria under combined tension and shear loadings, i.e., for a mixed mode stress field. This crack stability criterion is governed by either the maximum circumferential stress at the crack tip [3] or at a specified distance from the crack tip [4-6], the maximum energy release rate [7,8], and the minimum strain energy density factor surrounding the crack tip [9,10] or at a specified distance from the crack tip [11]. Sih [12] extended the minimum strain energy density factor criteria to rapidly propagating cracks for predicting the crack branching angle with a singular stress field.

Rossmanith [13] and the authors [14-16] have shown that the nonsingular component in the stress acting parallel to the crack path has considerable influence on the directional stability of a moving crack and incorporated this component for estimating the curving and bifurcation angles. The additional higher order terms in the crack tip stresses, which are used to account for the spread of advanced cracks, are the cause of incipient branching in brittle materials, and enlarge the fracture process zone which results in roughening of the fracture surface. The presence of unsuccessful multiple cracks or crack interaction with the stress waves [17-19] under mode I loading are often associated with the slight unsymmetry in the fringe patterns of the dynamic photoelastic experiments of rapidly propagating cracks. This unsymmetry in the fringe pattern was modeled by Rossmanith [17] and the authors [19] by adding the higher order terms of mode I and mode II stress components to the mode I singular crack tip stress field. This inevitable involvement of the higher order terms forms the basis of the dynamic fracture analysis in this paper and the prediction of crack-growth direction of a constant crack velocity using the strain energy density factor, $r_c(dW/dV)$, criterion.

DYNAMIC MIXED MODE CRACK TIP STRESS FIELDS

The crack tip dynamic state of stresses under mixed mode conditions was given by Nishioka and Atluri [20] in terms of the local rectangular (x,y) and polar (r,θ) coordinates. The three rectangular stress components under mode I and mode II conditions are given as:

$$\begin{bmatrix}\sigma_{xx}\\ \sigma_{yy}\\ \sigma_{xy}\end{bmatrix} = \sum_{n=1}^{\infty} A_{In}\frac{B_I(c)}{\sqrt{2\pi}}\frac{n(n+1)}{2}\begin{bmatrix}(1+2S_1^2-S_2^2)r_1^{(\frac{n}{2}-1)}\cos(\frac{n}{2}-1)\theta_1-2h(n)r_2^{(\frac{n}{2}-1)}\cos(\frac{n}{2}-1)\theta_2\\ -(1+S_2^2)r_1^{(\frac{n}{2}-1)}\cos(\frac{n}{2}-1)\theta_1+2h(n)r_2^{(\frac{n}{2}-1)}\cos(\frac{n}{2}-1)\theta_2\\ -2S_1r_1^{(\frac{n}{2}-1)}\sin(\frac{n}{2}-1)\theta_1+\frac{(1+S_2^2)}{S_2}h(n)r_2^{(\frac{n}{2}-1)}\sin(\frac{n}{2}-1)\theta_2\end{bmatrix}$$

$$+\sum_{n=1}^{\infty} A_{IIn}\frac{B_{II}(c)}{\sqrt{2\pi}}\frac{n(n+1)}{2}\begin{bmatrix}(1+2S_1^2-S_2^2)r_1^{(\frac{n}{2}-1)}\sin(\frac{n}{2}-1)\theta_1-2h(\bar{n})r_2^{(\frac{n}{2}-1)}\sin(\frac{n}{2}-1)\theta_2\\ -(1+S_2^2)r_1^{(\frac{n}{2}-1)}\sin(\frac{n}{2}-1)\theta_1+2h(\bar{n})r_2^{(\frac{n}{2}-1)}\sin(\frac{n}{2}-1)\theta_2\\ 2S_1r_1^{(\frac{n}{2}-1)}\cos(\frac{n}{2}-1)\theta_1-\frac{(1+S_2^2)}{S_2}h(\bar{n})r_2^{(\frac{n}{2}-1)}\cos(\frac{n}{2}-1)\theta_2\end{bmatrix} \quad (1)$$

where

$$S_1^2 = 1-\frac{C^2}{C_1^2} \quad ; \quad S_2^2 = 1-\frac{C^2}{C_2^2}$$

$$B_I(c) = \frac{1+S_2^2}{D(C)} \quad ; \quad B_{II}(c) = \frac{2S_2}{D(C)}$$

$$D(c) = 4S_1S_2 - (1+S_2^2)^2$$

$$
h(n) = \begin{cases} \dfrac{2S_1S_2}{1+S_2^2} & : n \text{ odd} \\[2ex] \dfrac{1+S_2^2}{2} & : n \text{ even} \end{cases}
$$

$$
r_1^{\,2} = x^2 + S_1^{\,2}y^2 \qquad \tan\theta_1 = S_1\tan\theta
$$

$$
r_2^{\,2} = x^2 + S_2^{\,2}y^2 \qquad \tan\theta_2 = S_2\tan\theta
$$

$$
h(\bar{n}) = h(n+1) \qquad r^2 = x^2 + y^2
$$

r and θ are the polar coordinates with the origin at the moving crack tip, C, C_1, and C_2 are the crack velocity, dilatational and distortional wave velocities, respectively.

The general solution expressed in Equation (1) yields the singular stresses when $n = 1$, i.e., $A_{I1} = K_I$ and $A_{II1} = K_{II}$, which are stress intensity factors of mode I and mode II, respectively. The constant stress, σ_{ox}, is related to the higher order term (HOT) for $n = 2$.

$$
\sigma_{ox} = \frac{6B_I(c)(S_2^2-S_1^2)}{\sqrt{2\pi}} A_{I2} \tag{2}
$$

$$
A_{II2} = 0
$$

DYNAMIC STRAIN ENERGY DENSITY FACTOR CRITERION

The strain energy density factor, r_c (dW/dV), criterion developed by Sih [9] is based on the local density of the strain energy field at a core radius r_c from the crack tip. It assumes that fracture initiates when r_c(dW/dV) reaches a critical value of $[r_c(dW/dV)]_c$.

The elastic strain energy density, W, per unit volume, V, of the material is:

$$\frac{dW}{dV} = \frac{1+\nu}{2E} [(\sigma_{xx}{}^2 + \sigma_{yy}{}^2 + \sigma_{zz}{}^2) - \frac{\nu}{1+\nu} (\sigma_{xx} + \sigma_{yy} + \sigma_{zz})^2 + 2\sigma_{xy}{}^2] \quad (3)$$

for plane strain condition:

$$\sigma_{zz} = \nu(\sigma_{xx} + \sigma_{yy}) \quad (4)$$

and thus

$$\frac{dW}{dV} = \frac{1+\nu}{2E} [(1-\nu)(\sigma_{xx}{}^2 + \sigma_{yy}{}^2) - 2\nu(\sigma_{xx}\sigma_{yy}) + 2\sigma_{xy}{}^2] \quad (5)$$

where E and ν are the modulus of elasticity and Poisson's ratio, respectively.

As discussed earlier, for n = 2 the first nonsingular term exists only in σ_{xx}, stress component of mode I loading and is zero in all other components of mode I and mode II crack tip stress fields. These and other higher order terms for $n \geq 2$, on the strain energy density factor surrounding the crack tip are believed to influence the spreading of advanced cracks which turn leads to crack curving and branching. By denoting the energy density function (dW/dV) in the presence of higher order terms as $(dW/dV)_n$, the intensity of the strain energy density factor for the state of plane strain at a critical distance, r_c, can be written for as: $r_c(dW/dV)_n$. The subscript index, n, indicates the number of the terms considered in determining the strain energy density factor. By using Equations (1) through (5) and evaluating for n=1, the strain energy density factor, S, became:

$$S = [a_{11} A_{I1}{}^2 + 2a_{12} A_{I1} A_{II1} + a_{22} A_{II1}{}^2] \quad (6)$$

The coefficients a_{ij} depend upon C, C_1, C_2 and Poisson's ratio, ν. The fracture criterion based on the minimum strain energy density factor notes that the crack will extend to the location of the minimum strain energy density factor, $[r_c(dW/dV)]_{min}$. In the presence of higher order terms, strain energy density factor, criterion can be written as:

$$\frac{d[r_c(\frac{dW}{dV})]_n}{d\theta} = 0 \text{ at } \theta = \theta_c \qquad (7)$$

The half crack branching angle, θ_c, at which $[r_c dW/dV]_n$ possesses stationary values, can be obtained from Equation (7). As a check on the accuracy of Equation (5) and (7), the dynamic $r_c(dW/dV)$ should coincide with its static value in Reference [12], when the crack velocity c--> 0 for n=1.

NUMERICAL RESULTS

In order to study the variation of the strain energy density factor with angular orientation, the theoretical (dW/dV) values were computed for each 0.25 degrees, using a Poisson's ratio, ν = 0.36, Youngs Modulus, E = 3.74 GPa, critical radius r_c = 1.3mm, $A_{I1} = K_I = 1$ MPa$\sqrt{m}$, and $K_{II}/K_I = 0$ value. Static strain energy density factor was approximated by setting $C = 0.01C_2$ in Equations (1) and (7) where the results agreed well with that of References [12,13].

Crack velocities of C/C_2 = 0.01 to 0.8 were chosen to generate the dynamic strain energy density factor in the vicinity of the crack tip. The representative static and dynamic strain energy density factor distributions in the vicinity of the crack tip at a distance r_c = 1.3 mm are shown in Figure 1 for $A_{12}<0$, $A_{I2} = 0$, and $A_{I2}>0$ under mode I loading.

Figure 2 shows the angular variation of static and dynamic ($r_c dW/dV$) with the third higher order term A_{I3} which is compressive in nature, in addition to remote stress under pure mode I loading (i.e., $K_{II} = 0$). Figure 2(a) shows the strain energy density factor distribution for A_{I2} = -0.25 and A_{I3} = -0.3 for ν = 0.36 and Figure 2(b) represents the distribution of strain energy density factor for A_{12} = 0.25 and A_{13} = -0.3. The minimum value of strain energy density factor is almost constant within $\pm 10^o$ for $A_{12} < 0$ at lower crack velocities. However, the minimum strain energy density factor for $A_{12} > 0$ at lower crack velocities yields minimum $r_c(dW/dV)$ at greater than $\pm$ 30^o when crack velocity $C/C_2 \geq 0.5$. This is not surprising since the compressive remote stress stabilizes the crack path and the tensile stress enhances the directional instability of a propagating crack.

Figure 3 shows the angular distribution of dilatational and distortional strain energy density factors for the strain energy density factors in Figure 1 for A_{I1}= 1.0. It can be observed that the energy is constant between ± 13 degrees for lower crack velocities and the maximum magnitudes of the distortional energy and corresponding dilatational energy are minimum at $C/C_2 \leq$ 0.5. The minimum or maximum spread of dilational and distortional energy is constant within the ± 13 degrees angular region, respectively. A similar observation was made when we added A_{13} term to the stress field.

Figure 4 shows the branching angle versus crack velocity corresponding to a singular stress field with varying Poisson's ratio. The minimum strain energy density occured at angle θ = 0 for crack velocities $C/C_1 \leq 0.46$; it becomes non-zero for $C/C_1 > 0.46$. Note that the branching angle increased with increasing crack velocities. However, at higher velocities, the difference in branching angle is very small regardless of the difference in magnitudes of Poisson's ratio.

Table 1 shows the predicted crack branching angles using only the singular stress field with critical crack velocities of various materials represented by Poisson's ratio. These results suggest that the branching angle is very sensitive to the Poisson's ratio, ν. Note that the branching angle of ± 11 to ± 23 degrees occurred in these materials within the crack velocity range of C/C_2 = 0.47 to 0.64, which is higher than the experimentally observed crack velocities [1] irrespective of the material used. The discrepancy between the experimental observation and theory can be partly attributed to the finite geometry and boundary effects which influences all singular and higher order terms in the crack tip stress field. In the following, some representative values of the higher order terms (HOT) are used to show the difference in the predicted branching angles with HOT and without HOT in the stress field.

Figure 5 shows the branching angle versus the crack velocities for ν = 0.33, in the presence of higher order terms under the pure mode I loading condition. The addition of positive higher order terms enhanced the branching angle while negative higher order terms suppressed branching. The crack is directionally stable even at higher crack velocities of $C/C_2 = 0.6$ in the presence of negative HOT terms. Also, at higher crack velocities, the resulting branching angle is not influenced by the higher order terms, with differences of nearly 8 degrees.

Quite often the dynamic photoelastic fringe patterns associated with a propagating curved crack exhibits a slight unsymmetry in isochromatics under mode I loading. This unsymmetry in isochromatics is modeled by adding the mode II higher order terms, without the model II singular term. Since the applied remote load is only mode I loading, it is appropriate to disregard the singular term and add only A_{II3} term as was demonstrated previously in References [18,19].

Figure 6(a) shows the angular distribution of the strain energy density factor for crack velocities of C/C_2 = 0.01 to 0.8 and $A_{I2} = -0.25$, $A_{I3} = 0.3$, and $A_{II3} = -0.3$ for $\nu = 0.36$. The $r_c(dW/dV)_3$ distribution is slightly unsymmetric at lower crack velocity and increased at higher crack velocities. For a crack velocity of $0.4 \leq C/C_2 \geq 0.7$, the minimum strain energy density factor is located at about 20^o but at $C/C_2 = 0.8$, the minimum strain energy density factor occurs assymmetrically at about 55 and 60^o. Reversing the sign of A_{II3} from negative to positive in Figure 6(b) simply reverses the peaks in the strain energy density factor distribution. At lower crack velocities the positive higher order terms of mode II stress field enhances crack kinking and unsymmetric crack branching could occur at higher crack velocities. Therefore, for $A_{II3} < 0$, a positive kinking angle is obtained while for $A_{II3} > 0$, a negative kinking angle results. This effect is similar to the presence of positive and negative mode II stress intensity factors, respectively. The series of experimentation shows that branching could occur even in the presence of K_{II} at higher crack velocities.

Qualitative results of crack branching angles are presented in the following for Poisson's ratio of ν = 0.25, 0.29, and 0.33 for A_{I1} = 1.0, A_{I2} = -0.25, A_{I3} = 0.3 and higher order terms involving mode II nonsingular terms of A_{II1} = 0, A_{II2} = 0, and A_{II3} = 0.3. Table 2 shows the effect of HOT on crack branching angles for varying crack velocities. At lower crack velocities of $C/C_2 \leq 0.6$, the mode II higher order terms contributed to crack kinking and branched asummetrically at higher velocities. This observation is consistent with the present results in that the HOT effect is negligible at higher crack velocities. An enhanced branching angle also is clearly observed at higher velocities irrespective of the number of higher order terms present. Positive higher order terms enhanced magnitudes of the branching angle at all crack velocities. However, the crack branching angle was always 0 degree when $C/C_2 \leq$ 0.4 for all compressive or negative higher order terms.

Representative experimental crack branching data associated with running cracks in Homalite-100, polycarbonate, steel, aluminum [21] and glass were evaluated and presented in Table 3. There is good agreement between measured and predicted angles using higher order terms, whereas significant differences are observed when HOT terms were not used.

CONCLUSIONS

(1) The minimum value of $r_c(dW/dV)$ strongly depends on the first nonsingular stress, σ_{ox}, for a given Poisson's ratio under any mode of deformation. It also depends strongly on the crack velocity and varies systematically with the nonsingular stresses.

(2) For small values of $C/C_2 \leq 0.4$, the fracture angle θ_c, is found to be 0 for all negative higher order terms of mode I loading and $\theta_c \neq 0$ for all positive values of HOT, irrespective of crack velocity. Negative higher order terms suppresses the crack extension angle θ_c whereas positive HOT always enhances the θ_c, regardless of the Poisson's ratio.

(3) Depending on the test conditions and the shape of the fractured specimens, theoretically predicted angle could deviate from experimentally measured fracture angles when the second order term is neglected.

ACKNOWLEDGEMENT

The work reported here was obtained under ONR Contract No. N00014-76-C-0000 NR 064-478. The authors wish to acknowledge the support and encouragement of Dr. Y. Rajapakse, ONR, during the course of this investigation.

REFERENCES

1. M. Ramulu and A.S. Kobayashi "Mechanics of Crack Curing and Branching - An Elastodynamic Analysis," International Journal of Fracture, Vol. 27, No. 3-4, 187-201, 1985.

2. Dally, J.W., "Dynamic Photoelastic Studies of Fracture," Exp. Mech., 19, 349-367, 1979.

3. Erdogan, F., and G.C. Sih, "On the crack extension in plates under plane loading and transverse shear," J. Basic Engineering, Trans. ASME, 88, Ser. D., 519-527, 1963.

4. Williams, J.G., and P.D. Ewing, "Fracture under complex stress - The angled crack problem," Int. J. Fract. Mech., 8, 441-446, 1982.

5. Finnie, I., and A. Saith, "A note on the angled crack problem and the directional stability of crack," Int. J. Fracture, 9, 484-486, 1979.

6. Eftis, J., N. Subramanian, and H. Liebowitz, "Crack Boarder Stress and Displacement Equations Revisited," Eng. Frac. Mech., 9, 189-210, 1979.

7. Palaniswamy, K., and E.G. Knauss, "Propagation of a crack under general in-plane tension," Int. J. Fract. Mech., 8, 114-117, 1982.

8. Hussain, M.A., Sl.L. Pu, and J. Underwood, "Strain Energy Release Rate for a Crack Under Combined Mode-I and Mode-II," ASTM STP 560, 2-28, 1974.

9. Sih, G.C., "Some Basic Problems in Fracture Mechanics and New Concepts," Eng. Fract. Mech., 5, 365-377, 1983.

10. Sih, G.C., "Strain Energy Density Factor Applied to Mixed Mode Crack Problems," Int. J. Fract. Mech., 10, 305-321, 1974.

11. Sih, G.C., and M.E. Kipp, "Fracture under complex stress - The angled crack problem," Discussion, Int. J. Fract., 10, 261-265, 1984.

12. Sih, G.C., "Dynamic Crack Problems: Strain Energy Density Frcture Theory," Elastodynamic Crack Problems, ed. by G.C. Sih, Vol. 4, 17-37, Noordhoff, Leyden, 1977.

13. Rossmanith, H.P., "Crack Propagation and Branching," Proc. Symp. on Absorbed Spec. Energy/Strain Energy Density, ed. by G.C. Sih, E. Czoboloy, and G. Gillemot, Akademial Kiado, Budapest, 283-294, 1982.

14. Ramulu, M., and A.S. Kobayashi, "Dynamic Crack Curving - A Photoelastic Evaluation," Experimental Mechanics, 23, 1-9, 1983.

15. Ramulu, M., A.S. Kobayashi, and B.S.-J. Kang, Dynamic Crack Branching - A Photoelastic Evaluation, Fracture Mechanics (15th), ASTM. STP, 833, 130-142, 1984.

16. Ramulu, M., and A.S. Kobayashi, "Strain Energy Density Fracture Criterion in Elastodynamic Mixed Mode Crack Propagation," Eng. Fract. Mech., 18, 1087-1098, 1983.

17. Rossmanith, H.P., "How Mixed is Dynamic Mixed-Mode Crack Propagation? - A Dynamic Photoelastic Study," J. Mech. Phys. Solids, 31, 251-260, 1983.

18. Rossmanith, H.P., and A. Shukla, "Dynamic Photoelastic Investigation of Interaction of Stress Waves with Running Cracks," Exp. Mech., 21, 415-422, 1981.

19. Ramulu, M., Kobayashi, A.S. and Barker, D, "Analysis of Dynamic Mixed Mode Isochromatics," to be published in Experimental Mechnics.

20. Nishioka, T., and S.N. Atluri, "Path Independent Integrals, Energy Release Rates, and General Solutions of Near-Tip Fields in Mixed Mode Dynamic Fracture Mechanics," Eng. Fract. Mechanics, 17, 1-22, 1983.

21. Ramulu, M., Kobayashi, A.S., and Kang, B.S.J., "Dynamic Crack Curving and Branching in Line-Pipe." ASME J. of Pressure Vessel Technology, Vol. 104, 317-322, 1982.

ldk:232

Table 1

CRACK BRANCHING VELOCITY AND INITIAL CRACK BRANCHING ANGLE FOR VARIOUS MATERIALS

ν	C_1/C_2	C/C_2	θ_c^* $(\pm)$	Remarks
0.22	1.669	0.470	17	
0.23	1.688	0.480	16	
0.24	1.709	0.490	15	
0.25	1.732	0.500	15	
0.26	1.756	0.510	15	
0.27	1.782	0.520	15	Glass (heavy flint)
0.28	1.809	0.540	22	
0.29	1.838	0.550	23	
0.30	1.870	0.560	23	
0.31	1.905	0.555	11	
0.32	1.944	0.570	17	
0.33	1.985	0.575	13	
0.34	2.031	0.590	19	Homalite-100, aluminum
0.35	2.082	0.600	19	Polycarbonate
0.36	2.138	0.605	16	
0.37	2.201	0.610	13	
0.38	2.273	0.620	14	
0.40	2.449	0.636	13	

ldk:232

TABLE 2

EFFECT OF MODE II HIGHER ORDER TERMS ON CRACK EXTENSION ANGLE

$A_{I1} = 1.0$, $A_{I2} = 0.25$, $A_{I3} = 0.3$ AND $A_{II3} = 0.3$*

Poisson's Ratio ν	Crack Velocity C/C_2	Crack Extension Angle Θ_c	Remarks
0.25	0.50	2.50	Crack kinking
	0.54	11.75	Crack kinking
	0.58	33.25	Crack kinking
	0.62	± 44.25	Branching
	0.66	± 51.00	Branching
	0.72	± 57.75	Branching
0.29	0.56	5.25	Crack kinking
	0.60	27.00	Crack kinking
	0.64	± 40.75	Branching
	0.70	± 52.00	Branching
0.33	0.58	3.0	Crack kinking
	0.64	30.25	Crack kinking
	0.70	± 47.00	Branching

* Crack extension angles are negative for $A_{II3} < 0$.

TABLE 3

MEASURED AND CALCULATED VALUES OF BRANCH ANGLE

Material	Crack Velocity C/C_2	r_c mm	Measured Branch Angle $2\ \Theta_c$	Predicted Angle $2\ \Theta_c$ Without Hot	Predicted Angle $2\ \Theta_c$ With Hot	Remarks
Steel	0.44	1.0	66	0	64	Pressurized pipe
Aluminum	0.14	1.3	88	0	84	Pressurized pipe
HOMALITE-100	0.10	1.3	52	0	52	WL-RDCB specimen
	0.46	1.3	50	0	47	Biaxially loaded Centrally notched specimen
	0.38	1.3	28	0	0	SEN specimen
Polycarbonate	0.45	0.75	34	0	0	SEN specimen

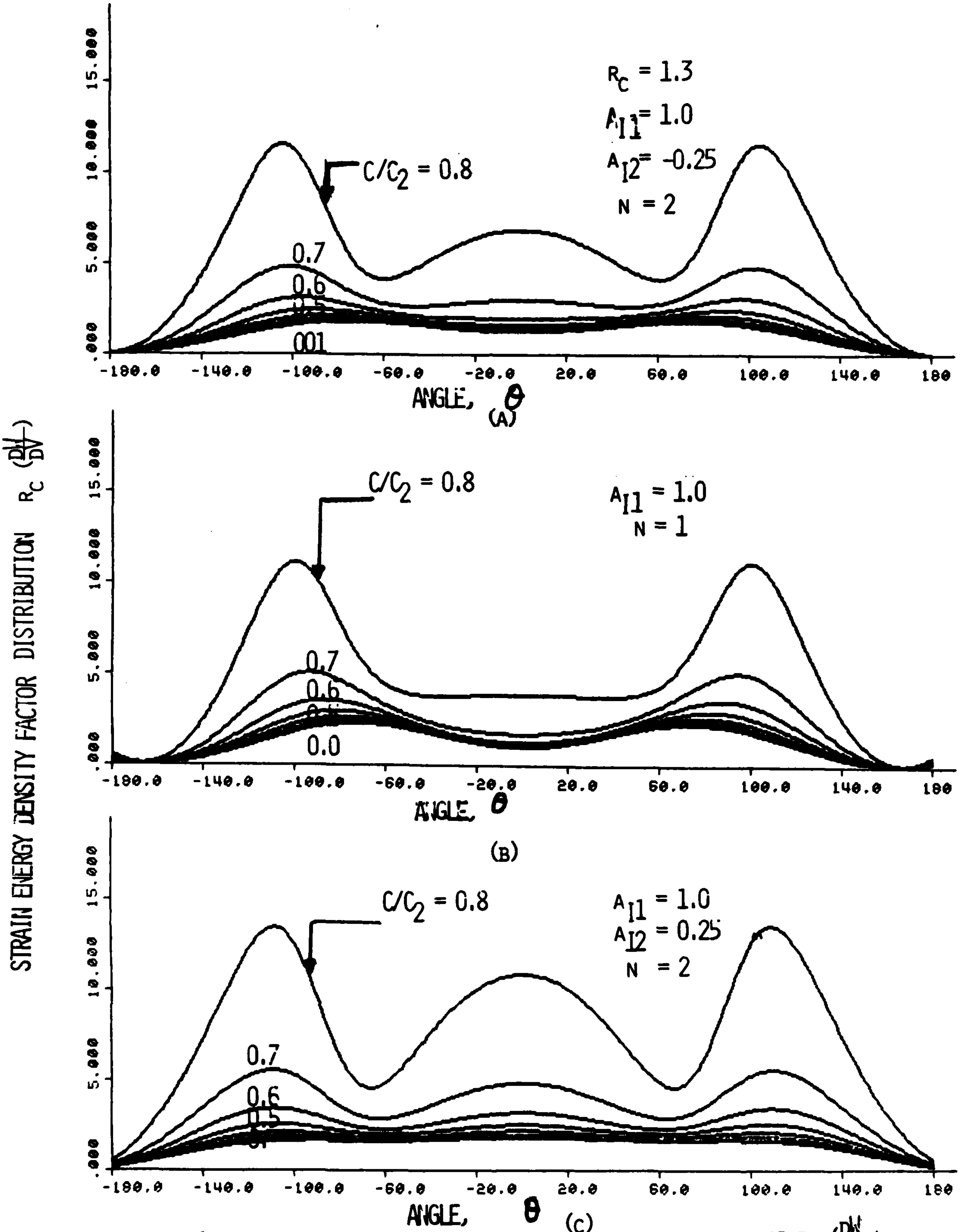

FIGURE 1. ANGULAR DISTRIBUTION OF STRAIN ENERGY DENSITY FACTOR R_C $(\frac{DW}{DV})$ IN PRESENCE OF FIRST NONSINGULAR STRESS COMPONENT, σ_{OX}.

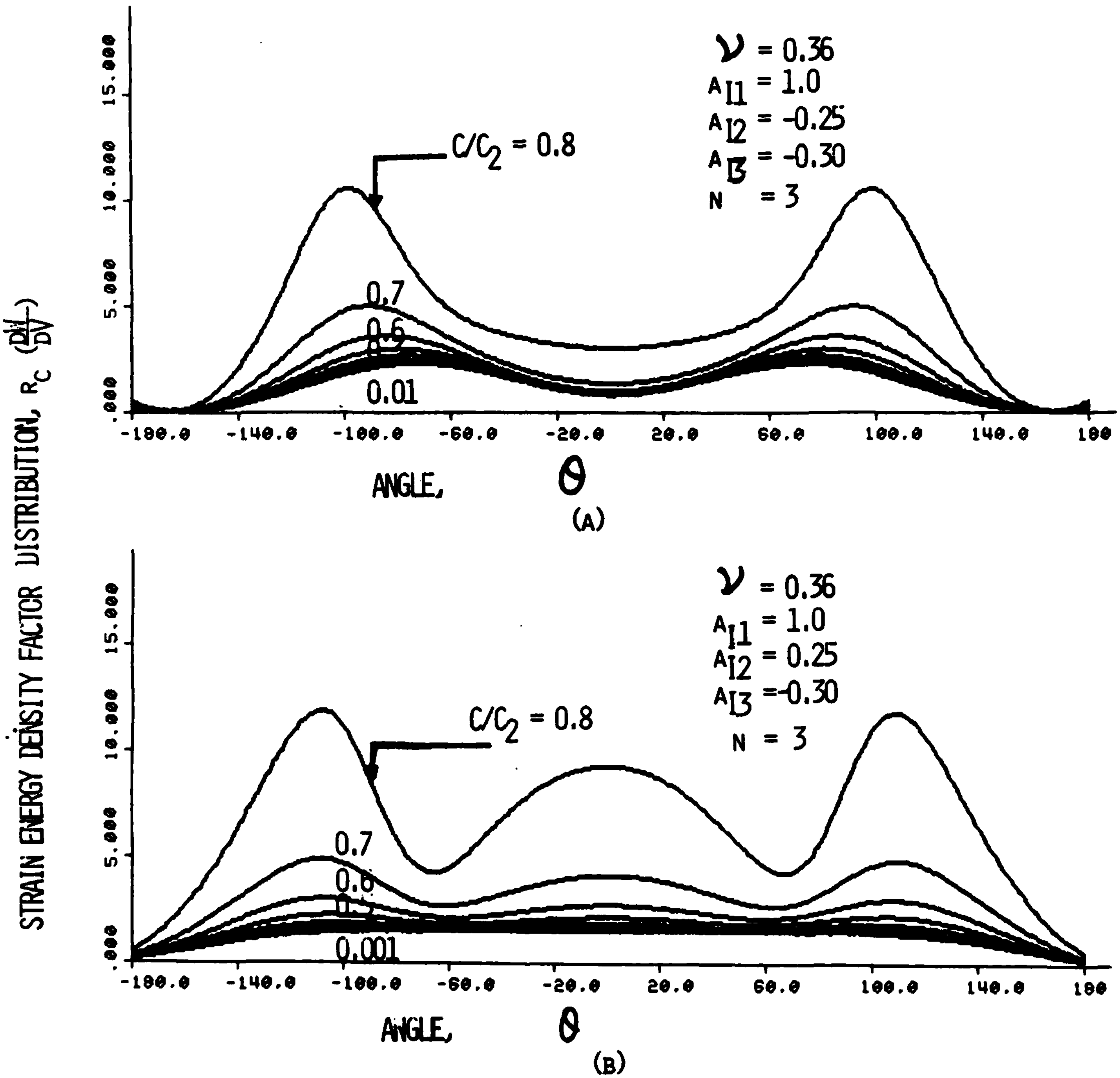

FIGURE 2. ANGULAR DISTRIBUTION OF STRAIN ENERGY DENSITY FACTOR R_C $(\frac{DW}{DV})$ IN PRESENCE OF HIGHER ORDER TERMS UNDER PURE MODE I LOADING.

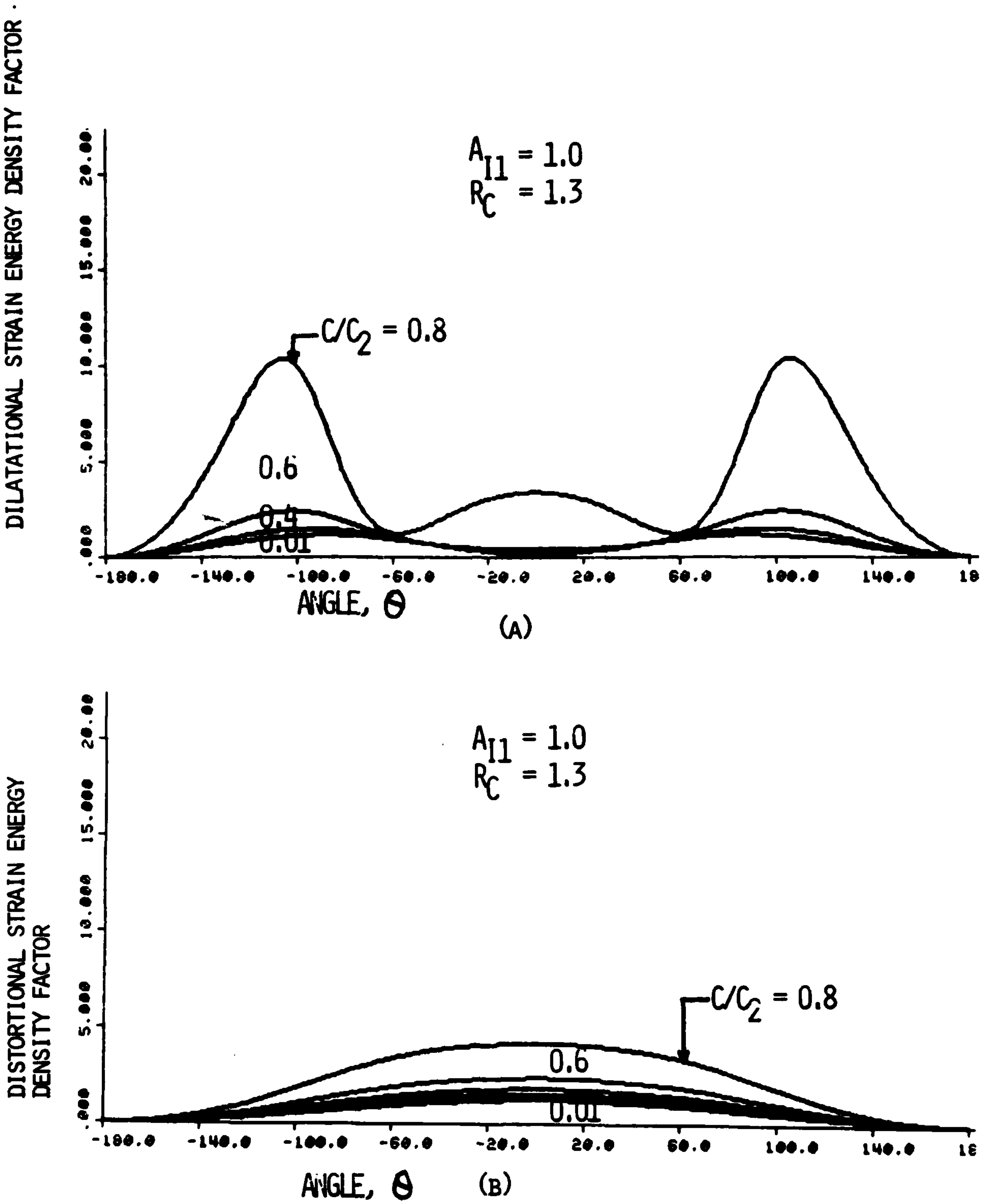

FIGURE 3. ANGULAR DISTRIBUTION DILATIONAL AND DISTORTIONAL STRAIN ENERGY DENSITY FACTORS UNDER SINGULAR STRESS FIELD.

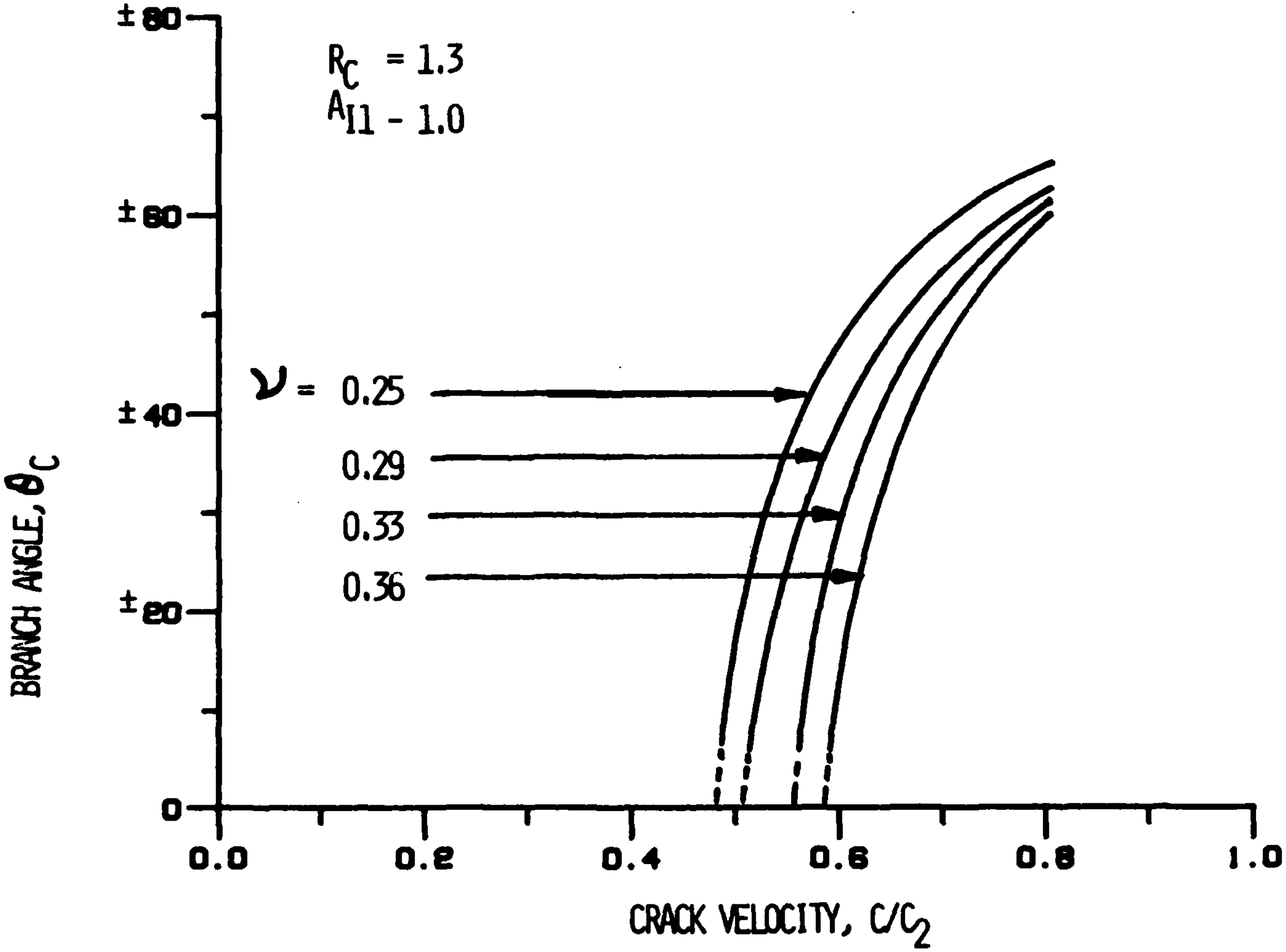

FIGURE 4. EFFECT OF POISSON'S RATIO, , ON CRACK BRANCHING ANGLE UNDER MODE I SINGULAR STRESS FIELD CONDITION.

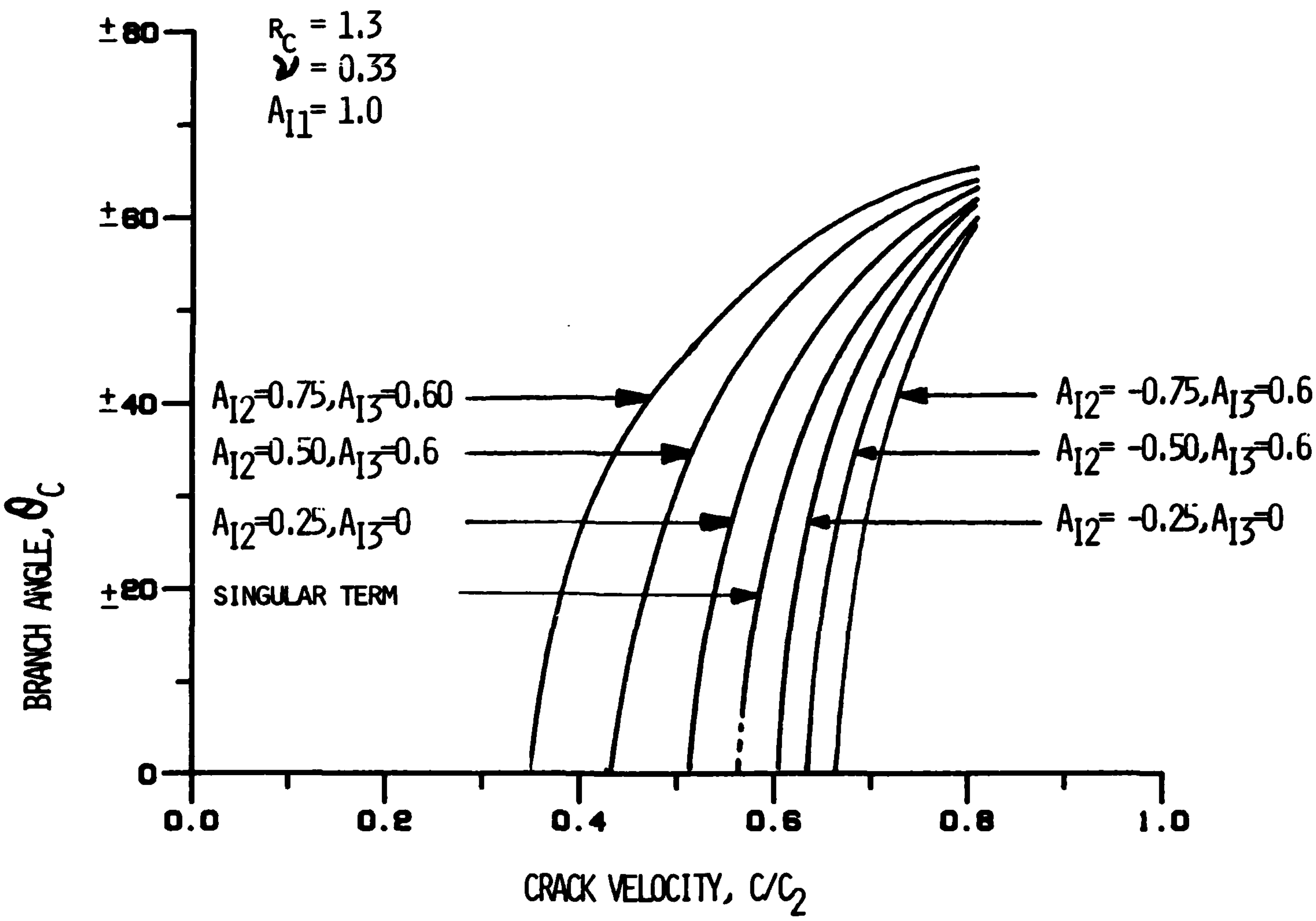

FIGURE 5. EFFECT OF MODE I HIGHER ORDER TERMS (HOT) ON CRACK BRANCHING ANGLE

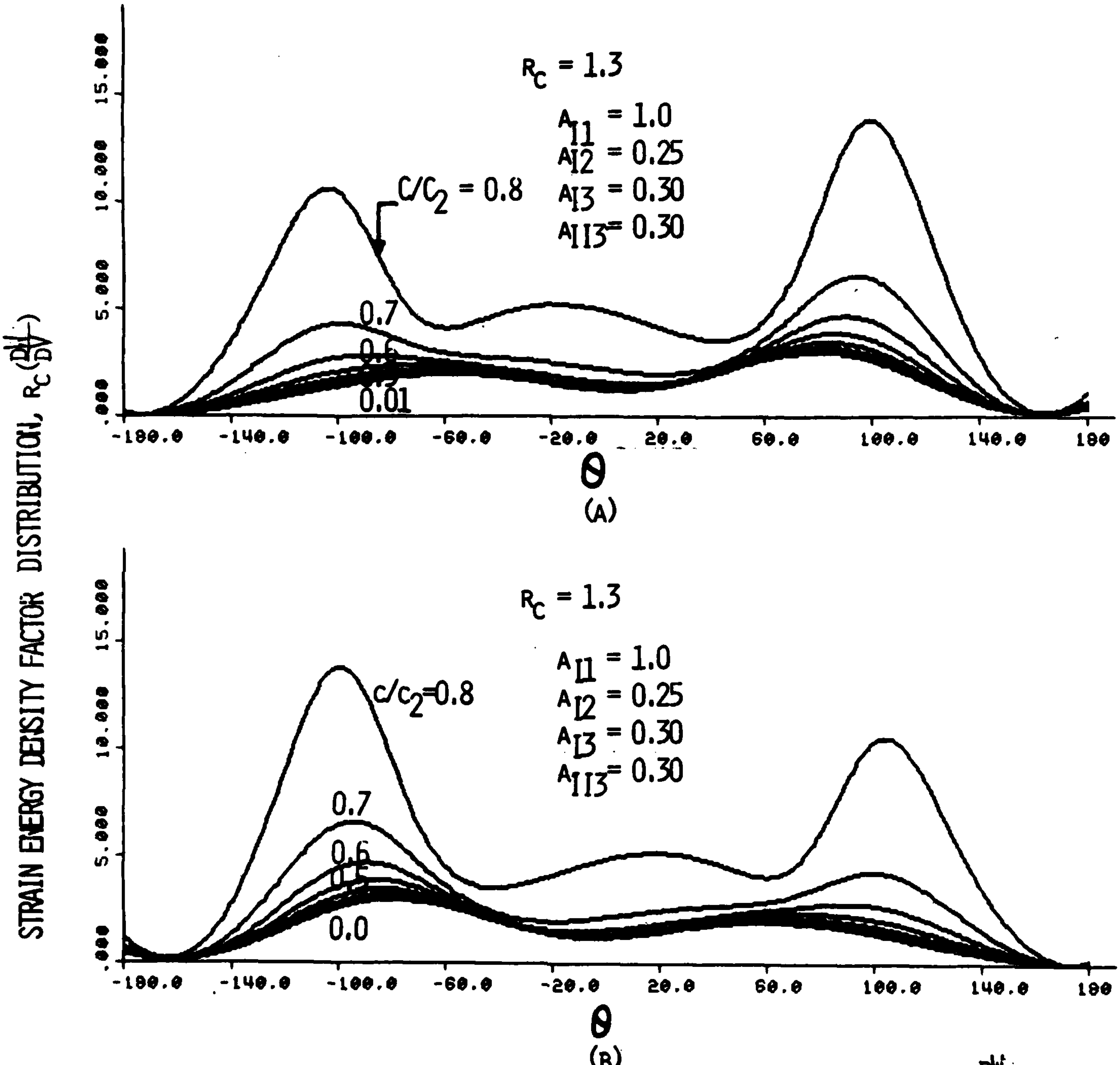

FIGURE 6. ANGULAR DISTRIBUTION OF STRAIN ENERGY DENSITY FACTOR, R_C $(\frac{DW}{DV})$ IN PRESENCE OF MODE I AND MODE II HIGHER ORDER TERMS.

Part 1 - Government
Administrative and Liaison Activities

Office of Naval Research
Department of the Navy
Arlington, VA 22217
Attn: Code 474 (2)
471
200

Director
Office of Naval Research
Branch Office
666 Summer Street
Boston, MA 02210

Director
Office of Naval Research
Branch Office
536 South Clark Street
Chicago, IL 60605

Director
Office of Naval Research
Branch Office
1030 East Green Street
Pasadena, CA 91106

Naval Research Laboratory (6)
Code 2627
Washington, D.C. 20375

Defense Documentation Center (12)
Cameron Station
Alexandria, Virginia 22314

Navy

Undersea Explosion Research Division
Naval Ship Research and Development
Center
Norfolk Naval Shipyard
Portsmouth, VA 23709
Attn: Dr. E. Palmer, Code 177

Navy (Con't.)

Naval Research Laboratory
Washington, D.C. 20375
Attn: Code 8400
8410
8430
8440
6300
6390
6380

David W. Taylor Naval Ship Research
and Development Center
Annapolis, MD 21402
Attn: Code 2740
28
281

Naval Weapons Center
China Lake, CA 93555
Attn: Code 4062
4520

Commanding Officer
Naval Civil Engineering Laboratory
Code L31
Port Hueneme, CA 93041

Naval Surface Weapons Center
White Oak
Silver Spring, MD 20910
Attn: Code R-10
G-402
K-82

Technical Director
Naval Ocean Systems Center
San Diego, CA 92152

Navy Underwater Sound
Reference Division
Naval Research Laboratory
P.O. Box 8337
Orlando, FL 32806

Navy (Con't.)

Chief of Naval Operations
Department of the Navy
Washington, D.C. 20350
Attn: Code OP-098

Strategic Systems Project Office
Department of the Navy
Washington, D.C. 20376
Attn: NSP-200

Naval Air Systems Command
Department of the Navy
Washington, D.C. 20361
Attn: Code 5302 (Aerospace and Structures)
604 (Technical Library)
320B (Structures)

Naval Air Development Center
Warminster, PA 18974
Attn: Aerospace Mechanics
Code 606

U.S. Naval Academy
Engineering Department
Annapolis, MD 21402

Naval Facilities Engineering Command
200 Stovall Street
Alexandria, VA 22332
Attn.: Code 03 (Research & Development)
04B
045
14114 (Technical Library)

Naval Sea Systems Command
Department of the Navy
Washington, D.C. 20362
Attn: Code 05H
312
322
323
05R
32R

Navy (Con't.)

Commander and Director
David W. Taylor Naval Ship
Research and Development Center
Bethesda, MD 20084
Attn: Code 042
17
172
173
174
1800
1844
012.2
1900
1901
1945
1960
1962

Naval Underwater Systems Center
Newport, RI 02840
Attn: Dr. R. Trainor

Naval Surface Weapons Center
Dahlgren Laboratory
Dahlgren, VA 22448
Attn: Code G04
G20

Technical Director
Mare Island Naval Shipyard
Vallejo, CA 94592

U.S. Naval Postgraduate School
Library
Code 0384
Monterey, CA 93940

Webb Institute of Naval Architecture
Attn: Librarian
Crescent Beach Road, Glen Cove
Long Island, NY 11542

Army

Commanding Officer (2)
U.S. Army Research Office
P.O. Box 12211
Research Triangle Park, NC 27709
Attn: Mr. J. J. Murray, CRD-AA-IP

Army (Con't.)

Watervliet Arsenal
MAGGS Research Center
Watervliet, NY 12189
Attn: Director of Research

U.S. Army Materials and Mechanics
Research Center
Watertown, MA 02172
Attn: Dr. R. Shea, DRXMR-T

U.S. Army Missile Research and
Development Center
Redstone Scientific Information
Center
Chief, Document Section
Redstone Arsenal, AL 35809

Army Research and Development
Center
Fort Belvoir, VA 22060

NASA

National Aeronautics and Space
Administration
Structures Research Division
Langley Research Center
Langley Station
Hampton, VA 23365

National Aeronautics and Space
Administration
Associate Administrator for Advanced
Washington, D.C. 20546

Air Force

Wright-Patterson Air Force Base
Dayton, OH 45433
Attn: AFFDL (FB)
(FBR)
(FBE)
(FBS)
AFML (MBM)

Air Force (Con't.)

Chief Applied Mechanics Group
U.S. Air Force Institute of Technology
Wright-Patterson Air Force Base
Dayton, OH 45433

Chief, Civil Engineering Branch
WLRC, Research Division
Air Force Weapons Laboratory
Kirtland Air Force Base
Albuquerque, NM 87117

Air Force Office of Scientific Research
Bolling Air Force Base
Washington, D.C. 20332
Attn: Mechanics Division

Department of the Air Force
Air University Library
Maxwell Air Force Base
Montgomery, AL 36112

Other Government Activities

Commandant
Chief, Testing and Development Division
U.S. Coast Guard
1300 E Street, NW.
Washington, D.C. 20226

Technical Director
Marine Corps Development
and Education Command
Quantico, VA 22134

Director Defense Research
and Engineering
Technical Library
Room 3C128
The Pentagon
Washington, D.C. 20301

Other Government Activities (Con't.)

Dr. M. Gaus
National Science Foundation
Environmental Research Division
Washington, D.C. 20550

Library of Congress
Science and Technology Division
Washington, D.C. 20540

Director
Defense Nuclear Agency
Washington, D.C. 20305
Attn: SPSS

Mr. Jerome Persh
Staff Specialist for Materials
and Structures
OUSDR&E, The Pentagon
Room 3D1089
Washington, D.C. 20301

Chief, Airframe and Equipment Branch
FS-120
Office of Flight Standards
Federal Aviation Agency
Washington, D.C. 20553

National Academy of Sciences
National Research Council
Ship Hull Research Committee
2101 Constitution Avenue
Washington, D.C. 20418
Attn: Mr. A. R. Lytle

National Science Foundation
Engineering Mechanics Section
Division of Engineering
Washington, D.C. 20550

Picatinny Arsenal
Plastics Technical Evaluation Center
Attn: Technical Information Section
Dover, NJ 07810

Maritime Administration
Office of Maritime Technology
14th and Constitution Ave., NW.
Washington, D.C. 20230

PART 2 - Contractors and other Technical
Collaborators

Universities

Dr. J. Tinsley Oden
University of Texas at Austin
345 Engineering Science Building
Austin, TX 78712

Professor Julius Miklowitz
California Institute of Technology
Division of Engineering
and Applied Sciences
Pasadena, CA 91109

Dr. Harold Liebowitz, Dean
School of Engineering and
Applied Science
George Washington University
Washington, D.C. 20052

Professor Eli Sternberg
California Institute of Technology
Division of Engineering and
Applied Sciences
Pasadena, CA 91109

Professor Paul M. Naghdi
University of California
Department of Mechanical Engineering
Berkeley, CA 94720

Professor A. J. Durelli
Oakland University
School of Engineering
Rochester, MD 48063

Professor F. L. DiMaggio
Columbia University
Department of Civil Engineering
New York, NY 10027

Professor Norman Jones
The University of Liverpool
Department of Mechanical Engineering
P.O. Box 147
Brownlow Hill
Liverpool L69 3BX
England

Professor E. J. Skudrzyk
Pennsylvania State University
Applied Research Laboratory
Department of Physics
State College, PA 16801

UNCLASSIFIED

SECURITY CLASSIFICATION OF THIS PAGE (When Data Entered)

REPORT DOCUMENTATION PAGE — READ INSTRUCTIONS BEFORE COMPLETING FORM

Field	Entry
1. REPORT NUMBER	UWA/DME/TR-85/51
2. GOVT ACCESSION NO.	
3. RECIPIENT'S CATALOG NUMBER	
4. TITLE (and Subtitle)	Strain Energy Density Criteria for Dynamic Fracture and Dynamic Crack Branching
5. TYPE OF REPORT & PERIOD COVERED	Technical Report
6. PERFORMING ORG. REPORT NUMBER	UWA/DME/TR-85/51
7. AUTHOR(s)	M. Ramulu and A. S. Kobayashi
8. CONTRACT OR GRANT NUMBER(s)	N00014-85-K-0187
9. PERFORMING ORGANIZATION NAME AND ADDRESS	Dept. of Mechanical Engineering, FU-10 University of Washington Seattle, Washington 98195
10. PROGRAM ELEMENT, PROJECT, TASK AREA & WORK UNIT NUMBERS	
11. CONTROLLING OFFICE NAME AND ADDRESS	Office of Naval Research Arlington, VA 22217
12. REPORT DATE	July 1985
13. NUMBER OF PAGES	19
14. MONITORING AGENCY NAME & ADDRESS (if different from Controlling Office)	
15. SECURITY CLASS. (of this report)	Unclassified
15a. DECLASSIFICATION/DOWNGRADING SCHEDULE	
16. DISTRIBUTION STATEMENT (of this Report)	Unlimited
17. DISTRIBUTION STATEMENT (of the abstract entered in Block 20, if different from Report)	
18. SUPPLEMENTARY NOTES	
19. KEY WORDS (Continue on reverse side if necessary and identify by block number)	Dynamic fracture, strain energy density factor, crack branching, crack kinking angle

AUG 1 5 1985

A

20. ABSTRACT (Continue on reverse side if necessary and identify by block number)

Dynamic extension of Sih's fracture criterion based on strain energy density factor, $r_c(dW/dV)$, is used to analyze dynamic crack propagation and branching. Influence of the nonsingular components, which are known as the higher order terms (HOT) in the crack tip stress field, on the strain energy density distribution at a critical distance surrounding the crack tip moving at constant crack velocity is examined. This $r_c(dW/dV)$ fracture criterion is then used to analyze available dynamic photoelastic results of crack branching and of engineering materials.

DD FORM 1 JAN 73 1473 EDITION OF 1 NOV 65 IS OBSOLETE
S/N 0102-014-6601

UNCLASSIFIED

SECURITY CLASSIFICATION OF THIS PAGE (When Data Entered)

85 8 9 180

Universities (Con't.)

Professor J. Klosner
Polytechnic Institute of New York
Department of Mechanical and
Aerospace Engineering
333 Jay Street
Brooklyn, NY 11201

Prof. R. A. Schapery
Texas A&M University
Department of Civil Engineering
College Station, TX 77843

Professor Walter D. Pilkey
University of Virginia
Research Laboratories for the
Engineering Sciences and
Applied Sciences
Charlottesville, VA 22901

Professor K. D. Willmert
Clarkson College of Technology
Department of Mechanical Engineering
Potsdam, NY 13676

Dr. Walter E. Haisler
Texas A&M University
Aerospace Engineering Department
College Station, TX 77843

Dr. Hussein A. Kamel
University of Arizona
Department of Aerospace and
Mechanical Engineering
Tucson, AZ 85721

Dr. S. J. Fenves
Carnegie-Mellon University
Department of Civil Engineering
Schenley Park
Pittsburgh, PA 15213

Dr. Ronald L. Huston
Department of Engineering Analysis
University of Cincinnati
Cincinnati, OH 45221

Universities (Con't.)

Professor G. C. M. Sih
Lehigh University
Institute of Fracture and
Solid Mechanics
Bethlehem, PA 18015

Professor Albert S. Kobayashi
University of Washington
Department of Mechanical Engineering
Seattle, WA 98105

Professor Daniel Frederick
Virginia Polytechnic Institute and
State University
Department of Engineering Mechanics
Blacksburg, VA 24061

Professor A. C. Eringen
Princeton University
Department of Aerospace and
Mechanical Sciences
Princeton, NJ 08540

Professor E. H. Lee
Stanford University
Division of Engineering Mechanics
Stanford, CA 94305

Professor Albert I. King
Wayne State University
Biomechanics Research Center
Detroit, MI 48202

Dr. V. R. Hodgson
Wayne State University
School of Medicine
Detroit, MI 48202

Dean B. A. Boley
Northwestern University
Department of Civil Engineering
Evanston, IL 60201

Universities (Con't.)

Professor P. G. Hodge, Jr.
University of Minnesota
Department of Aerospace Engineering
and Mechanics
Minneapolis, MN 55455

Dr. D. C. Drucker
University of Illinois
Dean of Engineering
Urbana, IL 61801

Professor N. J. Newmark
University of Illinois
Department of Civil Engineering
Urbana, IL 61803

Professor E. Reissner
University of California, San Diego
Department of Applied Mechanics
La Jolla, CA 92037

Professor William A. Nash
University of Massachusetts
Department of Mechanics and
Aerospace Engineering
Amherst, MA 01002

Professor G. Herrmann
Stanford University
Department of Applied Mechanics
Stanford, CA 94305

Professor J. D. Achenbach
Northwest University
Department of Civil Engineering
Evanston, IL 60201

Professor S. B. Dong
University of California
Department of Mechanics
Los Angeles, CA 90024

Professor Burt Paul
University of Pennsylvania
Towne School of Civil and
Mechanical Engineering
Philadelphia, PA 19104

Universities (Con't.)

Professor H. W. Liu
Syracuse University
Department of Chemical Engineering
and Metallurgy
Syracuse, NY 13210

Professor S. Bodner
Technion R&D Foundation
Haifa, Israel

Professor Werner Goldsmith
University of California
Department of Mechanical Engineering
Berkeley, CA 94720

Professor R. S. Rivlin
Lehigh University
Center for Application
of Mathematics
Bethlehem, PA 18015

Professor F. A. Cozzarelli
State University of New York at
Buffalo
Division of Interdisciplinary Studies
Karr Parker Engineering Building
Chemistry Road
Buffalo, NY 14214

Professor Joseph L. Rose
Drexel University
Department of Mechanical Engineering
and Mechanics
Philadelphia, PA 19104

Professor B. K. Donaldson
University of Maryland
Aerospace Engineering Department
College Park, MD 20742

Professor Joseph A. Clark
Catholic University of America
Department of Mechanical Engineering
Washington, D.C. 20064

Universities (Con't.)

Dr. Samuel B. Batdorf
University of California
School of Engineering
and Applied Science
Los Angeles, CA 90024

Professor Isaac Fried
Boston University
Department of Mathematics
Boston, MA 02215

Professor E. Krempl
Rensselaer Polytechnic Institute
Division of Engineering
Engineering Mechanics
Troy, NY 12181

Dr. Jack R. Vinson
University of Delaware
Department of Mechanical and Aerospace
Engineering and the Center for
Composite Materials
Newark, DE 19711

Dr. J. Duffy
Brown University
Division of Engineering
Providence, RI 02912

Dr. J. L. Swedlow
Carnegie-Mellon University
Department of Mechanical Engineering
Pittsburgh, PA 15213

Dr. V. K. Varadan
Ohio State University Research Foundation
Department of Engineering Mechanics
Columbus, OH 43210

Dr. Z. Hashin
University of Pennsylvania
Department of Metallurgy and
Materials Science
College of Engineering and
Applied Science
Philadelphia, PA 19104

Universities (Con't.)

Dr. Jackson C. S. Yang
University of Maryland
Department of Mechanical Engineering
College Park, MD 20742

Professor T. Y. Chang
University of Akron
Department of Civil Engineering
Akron, OH 44325

Professor Charles W. Bert
University of Oklahoma
School of Aerospace, Mechanical,
and Nuclear Engineering
Norman, OK 73019

Professor Satya N. Atluri
Georgia Institute of Technology
School of Engineering and
Mechanics
Atlanta, GA 30332

Professor Graham F. Carey
University of Texas at Austin
Department of Aerospace Engineering
and Engineering Mechanics
Austin, TX 78712

Dr. S. S. Wang
University of Illinois
Department of Theoretical and
Applied Mechanics
Urbana, IL 61801

Industry and Research Institutes

Dr. Norman Hobbs
Kaman AviDyne
Division of Kaman
Sciences Corporation
Burlington, MA 01803

Argonne National Laboratory
Library Services Department
9700 South Cass Avenue
Argonne, IL 60440

Industry and Research Institutes (Con't.)

Dr. M. C. Junger
Cambridge Acoustical Associates
54 Rindge Avenue Extension
Cambridge, MA 02140

Dr. V. Godino
General Dynamics Corporation
Electric Boat Division
Groton, CT 06340

Dr. J. E. Greenspon
J. G. Engineering Research Associates
3831 Menlo Drive
Baltimore, MD 21215

Newport News Shipbuilding and
Dry Dock Company
Library
Newport News, VA 23601

Dr. W. F. Bozich
McDonnell Douglas Corporation
5301 Bolsa Avenue
Huntington Beach, CA 92647

Dr. H. N. Abramson
Southwest Research Institute
8500 Culebra Road
San Antonio, TX 78284

Dr. R. C. DeHart
Southwest Research Institute
8500 Culebra Road
San Antonio, TX 78284

Dr. M. L. Baron
Weidlinger Associates
110 East 59th Street
New York, NY 10022

Dr. T. L. Geers
Lockheed Missiles and Space Company
3251 Hanover Street
Palo Alto, CA 94304

Mr. William Caywood
Applied Physics Laboratory
Johns Hopkins Road
Laurel, MD 20810

Industry and Research Institutes (Con't.)

Dr. Robert E. Dunham
Pacifica Technology
P.O. Box 148
Del Mar, CA 92014

Dr. M. F. Kanninen
Battelle Columbus Laboratories
505 King Avenue
Columbus, OH 43201

Dr. A. A. Hochrein
Daedalean Associates, Inc.
Springlake Research Road
15110 Frederick Road
Woodbine,, MD 21797

Dr. James W. Jones
Swanson Service Corporation
P.O. Box 5415
Huntington Beach, CA 92646

Dr. Robert E. Nickell
Applied Science and Technology
3344 North Torrey Pines Court
Suite 220
La Jolla, CA 92037

Dr. Kevin Thomas
Westinghouse Electric Corp.
Advanced Reactors Division
P.O. Box 158
Madison, PA 15663

Dr. Bernard Shaffer
Polytechnic Institute of New York
Dept. of Mechanical and Aerospace
Engineering
333 Jay Street
Brooklyn,, NY 11021

END

FILMED

10-85

DTIC